https://doi.org/10.5194/hess-2021-520
Preprint. Discussion started: 26 October 2021

Hydrology and Earth System Sciences
Discussions

On the similarity of hillslope hydrologic function: a process-based approach

Fadji Z. Maina[1,2*], Haruko M. Wainwright[1], Peter James Dennedy-Frank[1], Erica R. Siirila-Woodburn[1]

[1] Energy Geosciences Division, Lawrence Berkeley National Laboratory 1 Cyclotron Road, M.S. 74R-316C, Berkeley, CA 94704, USA

[2]now at NASA Goddard Space Flight Center, Hydrological Sciences Laboratory, 8800 Greenbelt Rd, Greenbelt, 20771, MD, USA

*Corresponding Author: fadjizaouna.maina@nasa.gov

https://doi.org/10.5194/hess-2021-520
Preprint. Discussion started: 26 October 2021

Hydrology and Earth System Sciences
Open Access
EGU
Discussions

Abstract

Hillslope similarity is an active topic in hydrology because of its importance to improve our understanding of hydrologic processes and enable comparisons and paired studies. In this study, we propose a holistic bottom-up hillslope similarity classification based on a region's integrative hydrodynamic response quantified by the seasonal changes in groundwater levels. The main advantage of the proposed classification is its ability to describe recharge and discharge processes. We test the performance of the proposed classification by comparing it to seven other common hillslope similarity classifications. These include simple classifications based on the aridity index, topographic wetness index, elevation, land cover, and more sophisticated machine-learning classifications that jointly integrate all these data. We assess the ability of these classifications to identify and categorize hillslopes with similar static characteristics, hydroclimatic behaviors, land surface processes, and subsurface dynamics in a mountainous watershed, the East River, located in the headwaters of the Upper Colorado River Basin. The proposed classification is robust as it reasonably identifies and categorizes hillslopes with similar elevation, land cover, hydroclimate, land surface processes, and subsurface hydrodynamics (and hence hillslopes with similar hydrologic function). In general, the other approaches are good in identifying similarity in a single characteristic, which is usually close to the selected variable. We further demonstrate the robustness of the proposed classification by testing its ability to predict hillslope responses to wet and dry hydrologic conditions, of which it performs well when based on average conditions.

Keywords: Hillslope, similarity, seasonal groundwater variations, integrated hydrologic modeling, hillslope classification, hydrologic function

https://doi.org/10.5194/hess-2021-520
Preprint. Discussion started: 26 October 2021

Hydrology and Earth System Sciences
Discussions

1. Introduction

The ability to delineate areas into spatially defined regions for their use in characterizing hydrologic flow and transport behavior is important for several reasons, including the assessment, monitoring, and modeling of water quantity and quality. Hillslopes are the scale at which hydrologic flow and transport processes can be tractably and frequently measured. It is also the scale at which water transfer and travel time are quantified and the instrumentation, conceptualization, and modeling of hydrologic processes occur (Fan et al., 2019). While advancements have been made in the general understanding of hillslope dynamics over the last several decades, there is yet to be a globally agreed-upon classification system for this important scale of interest in hydrology. Hydrologic signatures within hillslopes are the results of several simultaneous and nonlinear above- and below-ground processes. The uniqueness of a given location's characteristics (for example, the topography, geology, vegetation, etc.) limits our ability to draw general hypotheses and to develop a similarity framework (Beven, 2000). Nevertheless, a classification is needed to provide guidance on catchments and hillslopes comparisons (McDonnell & Woods, 2004), paired studies (Andréassian et al., 2012; Bosch & Hewlett, 1982; Brown et al., 2005), and improve our understanding of the changes in hydrologic processes across the world. By simplifying the complexities of the hydrologic dynamics, classification provides a better understanding of these processes. Further, hillslope similarity grouping is potentially an important step toward developing reduced-order models and machine learning algorithms, where grouping regions based on their similarities or dissimilarities can substantially reduce computational costs (Chaney et al., 2018). The scaling of hillslope to catchment classifications can also be useful in the prediction of hydrologic behavior in ungauged basins (Sivapalan et al., 2003), an exceedingly important challenge.

https://doi.org/10.5194/hess-2021-520
Preprint. Discussion started: 26 October 2021

Classical definitions of hillslope similarity include the Topographic Wetness Index TWI (Beven & Kirby, 1979), which was proposed to quantify the topographic control on hydrology as topography plays a key role in the movement of water. Many other variants of this index have been later proposed to improve the definition of topographic similarity (Grabs et al., 2009; Hjerdt et al., 2004; Loritz et al., 2019). Other classifications include similarities based on hydroclimate (Carrillo et al., 2011), soil type and texture (Bormann, 2010), and land cover type (e.g., forest, urban, etc. (Wagener et al., 2007)). These indices assume that hillslopes with similar elevation and land cover will have similar hydrologic responses. However, given that hydrologic processes are governed by many characteristics of the hillslope, similarity patterns have also been proposed based on the simultaneous accounting of multiple landscape characteristics. These classifications are usually based on clustering which aims to integrate all these data layers to identify and categorize similar hillslopes (Aryal et al., 2002; Sawicz et al., 2011). These top-down classifications assume that areas with similar static characteristics will lead to similar hydrologic processes and functions. This often-overlooked assumption presumes that an apparent physical similarity equates to a similarity in hydrologic processes (Oudin et al., 2010). Other classifications use a bottom-up approach, where similarity is defined based on the hydrologic process or functional response of interest. A process-based classification enables the analysis of different hydrologic responses and the identification of the hydrologic function itself. It also allows the estimation of the "hidden" hillslope characteristics such as soil texture, and geology that may drive similar hydrologic responses (Carrillo et al., 2011). Among the process-based classification existing in the literature we can cite: the Péclet number characterizing the diffusive and advective transfer of water at hillslope scale (Berne et al., 2005; S. W. Lyon & Troch, 2007; Steve W. Lyon & Troch, 2010) and the catchment seasonal water balance (Berghuijs et al.,

https://doi.org/10.5194/hess-2021-520
Preprint. Discussion started: 26 October 2021

Hydrology and Earth System Sciences Discussions

2014). Other authors have derived hillslope similarities from subsurface flow dynamics (Harman & Sivapalan, 2009).

One challenge in developing a similarity framework is the inherent heterogeneity of a given hillslope. For example, hillslope Snow Water Equivalent (SWE) distribution can vary up to 300 mm; similarly, infiltration (I) and actual evapotranspiration (ET) rates can range over an order of magnitude within a single hillslope. Defining a single integrative measure that can capture this spatio-temporal variability is difficult. However, groundwater fluctuations are often tightly linked to seasonal changes in weather and have been shown to play an important role in surficial processes such as ET (Maina & Siirila-Woodburn, 2020; Maxwell & Condon, 2016). Thus, groundwater measures may serve as a good proxy for the aggregated hydrologic response. Groundwater dynamics could help overcome the issue of uniqueness of place because even if there are strong differences in the characteristics of the hillslope, the integrated response may be similar as some of the processes might not be important. Finally, the implications of groundwater changes are also important. For example, many regions are characterized by groundwater-dependent ecosystems or are hypothesized to have water table fluctuations affecting bedrock weathering rates and therefore the concentration and fluxes of metals and nutrients exports (e.g., Winnick et al., 2017).

In this study, we define a holistic bottom-up hillslope similarity framework based on a region's integrative hydrodynamic response quantified by the seasonal changes in groundwater levels, hereafter referred to as a region's *functional zonation*. A caveat to this approach is that groundwater dynamics are difficult to quantify, and their measurements are frequently scarce. Hence, there are very few studies that use this variable to develop a hillslope similarity framework (Aryal et al., 2002; S. W. Lyon & Troch, 2007). However, today, thanks to advances

Hydrology and Earth System Sciences Discussions

in integrated hydrologic modeling (Brunner & Simmons, 2012; Maxwell & Miller, 2005), accurate quantification of the groundwater dynamics at high resolution in both time and space, as well as their interaction with the key land surface processes and features, is now feasible. These models account for the two-way interactions between groundwater and land surface processes. Spatially resolved hydrologic flow models also enable us to jointly quantify other hydrologic variables of interest, namely trends in ET, SWE, and I. These variables may be useful to define functional zonation (i.e., areas with similar hydrologic functions) and can be constrained by measurements at ultra-high resolutions through aerial or remote sensing (i.e., drones, planes, or satellites).

We test the proposed hillslope similarity approach on the site of the Department of Energy's (DOE) Watershed Function Scientific Focus Area (SFA) located in the headwaters of the Upper Colorado River Basin. The East River watershed is not only representative of many headwater catchments in the western United States in terms of its spatial heterogeneity of above and below-ground characteristics but also serves as an important proxy of water quantity and quality trends which ultimately impact a large population of water supply in the western US (for municipal, agriculture, and industrial use). The East River mountainous headwater catchment, characterized by high spatial and temporal variabilities in above-ground and below-ground hydrologic responses (Hubbard et al., 2018), is a good candidate site to demonstrate our approach. We test the robustness of the proposed hillslope similarity framework by comparing it to seven other common hillslope similarity measures. These include approaches based on single data layers (aridity index (AI), TWI, elevation, and land cover) and more sophisticated machine-learning approaches that jointly integrate multiple input data layers such as elevation, land cover, and geology, and model outputs including ET, and SWE. We assess the ability of these

Hydrology and Earth System Sciences
Open Access
Discussions

approaches to identify and categorize hillslopes with similar characteristics (land cover and elevation), hydroclimate (precipitation and temperature), land surface processes (ET and SWE), and subsurface dynamics (soil saturation, water table depth, and seasonal changes in groundwater). We aim to provide answers to the following questions:

- What are the best classifications for identifying hillslopes with similar hydrologic functions?
- Is a similarity index based on the seasonal groundwater variations sufficient to capture all the complex processes taking place at a hillslope scale?

2. Methods

2.1. Numerical model

The integrated hydrologic model, ParFlow, solves the subsurface flow using the three-dimensional mixed form of the Richards equation (Richards, 1931) given by the following equation:

$$S_S S_W(\psi_P)\frac{\partial \psi_P}{\partial t} + \phi\frac{\partial S_W(\psi_P)}{\partial t} = \nabla.[K(x)k_r(\psi_P)\nabla(\psi_P - z)] + q_s \quad (1)$$

Where is S_S the specific storage [L^{-1}], $S_W(\psi_P)$ is the degree of saturation [-] associated with the subsurface pressure head ψ_P [L], t is the time [T], ϕ is the porosity [-], k_r is the relative permeability [-], z is the depth [L], q_s is the source/sink term [T^{-1}] and $K(x)$ is the saturated hydraulic conductivity [L T^{-1}] which is assumed to be a diagonal tensor with entries given as: $k_x(x)$, $k_y(x)$ and $k_z(x)$. We assumed in this work that the domain is isotropic, and that the tensor is equal to 1 for all the three directions at each cell of the discretized model. In the unsaturated zone, both S_W and k_r depend on the ψ. The relationships between S_W and k_r and ψ are described by the van Genuchten model (van Genuchten, 1980).

Overland flow (equation 2) is solved by the kinematic wave equation in two dimensions.

https://doi.org/10.5194/hess-2021-520
Preprint. Discussion started: 26 October 2021

Hydrology and Earth System Sciences
Discussions

$$-k(x)k_r(\psi_0)\nabla(\psi_0 - z) = \frac{\partial\|\psi_0,0\|}{\partial t} - \nabla.\vec{v}\|\psi_0,0\| - q_r(x) \tag{2}$$

Where ψ_0 is the ponding depth, $\|\psi_0, 0\|$ indicates the greater term between ψ_0 and 0, $\vec{v}$ is the depth averaged velocity vector of surface runoff [L T^{-1}], q_r is a source/sink term representing rainfall and evaporative fluxes [L T^{-1}] Surface water velocity at the surface in *x* and *y* directions, (υ_x) and (υ_y) respectively, is computed using the following set of equations:

$$\upsilon_x = \frac{\sqrt{S_{f,x}}}{m}\psi_0^{\frac{2}{3}} \text{ and } \quad \upsilon_y = \frac{\sqrt{S_{f,y}}}{m}\psi_0^{\frac{2}{3}} \tag{3}$$

Where $S_{f,x}$ and $S_{f,y}$ friction slopes along *x* and *y* respectively and m is the manning's coefficient. ParFlow employs a cell-centered finite difference scheme along with an implicit backward Euler scheme and the Newton Krylow linearization method to solve these nonlinear equations. The computational grid follows the terrain to mimic the slope of the domain (Maxwell, 2013).

ParFlow is coupled to the Community Land Model (CLM, (Dai et al., 2003)) which allows for the simulation of important land surface processes such as ET and SWE and the quantification of water leaving or entering the surface and subsurface (q_s and q_r respectively in the Richards and kinematic wave equations). CLM models the thermal processes by closing the energy balance at the land surface given by:

$$R_n(\theta) = LE(\theta) + H(\theta) + G(\theta) \tag{4}$$

Where $R_n$is the net radiation at the land surface [E/LT] a balance between the shortwave and longwave radiation, LE is the latent heat flux [E/LT] which captures the energy required to change the phase of water to or from vapor, H is the sensible heat flux [E/LT] and G is the ground heat flux [E/LT]. All terms are a function of θ, the water content, which is computed by ParFlow.

Computing the different components of the energy balance requires meteorological forcing, vegetative parameters, and soil moisture. The latter is computed by ParFlow using equations 1 and 2. Meteorological forcing includes precipitation, temperature, east to west and north to south wind speed, longwave and shortwave solar radiation, air pressure, and relative humidity. Vegetative parameters include maximum and minimum leaf area index, stem area index, aerodynamic roughness height, optical properties, stomatal physiology, roughness length, and displacement height. More details about the coupling between ParFlow and CLM as well as the equations governing the snow dynamics and *ET* can be found in the following papers: Jefferson et al., (2015); Maxwell & Miller, (2005); Ryken et al., (2020).

2.2. East River watershed model set-up

The East River watershed (Figure 1), located in the Upper Colorado Basin, is one of the two major tributaries that form the Gunnison River, which in turn accounts for just under half of the Colorado River's discharge at the Colorado-Utah border. The total area of this watershed is approximately 255 km^2 and the elevation varies from approximately 3900 to 2700 m. The watershed is characterized by strong heterogeneities in vegetation, geomorphology, and bedrock composition (Hubbard et al., 2018). The vegetation includes grasses, conifers, mixed conifers, aspens, and meadows and lies on a complex geologic terrain, which is comprised of a diverse collection of Paleozoic and Mesozoic sedimentary and unconsolidated rocks. The watershed is also characterized by a strong hydroclimate gradient. The average precipitation is 1200 mm/year while the average temperature is around 0°C. Because of its very low cold winter with temperature below 0°C, most of the winter precipitation is in the form of snow.

https://doi.org/10.5194/hess-2021-520
Preprint. Discussion started: 26 October 2021

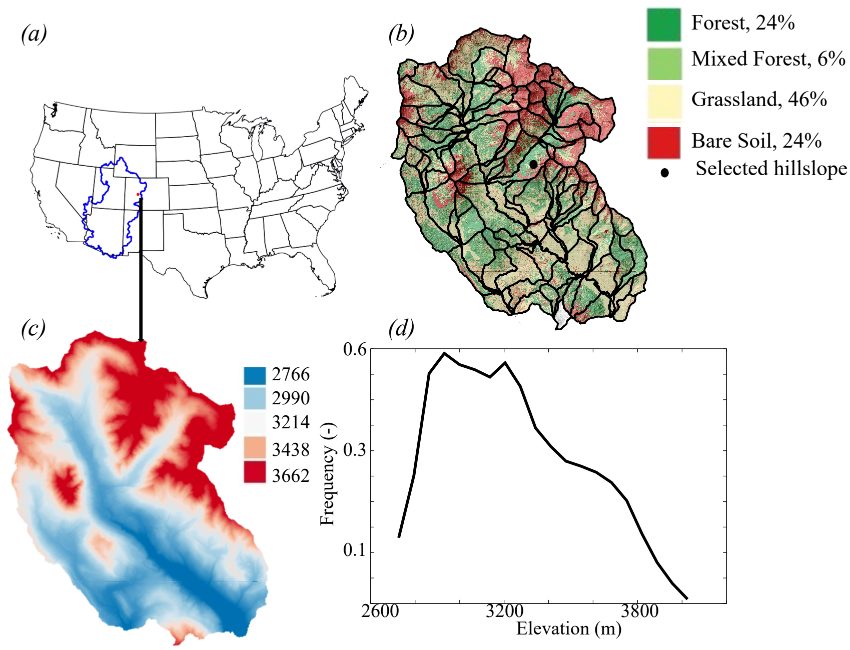

Figure 1: (a) location of the East River watershed, (b) land cover (NEON dataset, 2020), (c) LiDAR Digital elevation, and (d) elevation distribution within the East River.

ParFlow-CLM used here is based on a previous version of the East River watershed model, as described by Foster and Maxwell (2019). 5 layers constitute the model in the vertical direction with varying thickness from 0.1 m at the land surface to 21 m at the bottom of the domain. The land use and land cover are derived from the high-resolution airborne remote sensing NEON campaign (NEON dataset, 2020). From the hyperspectral spectrometer and LiDAR readings, 4 major types of land cover are grouped as follows: forests (i.e. conifers and aspens), mixed forests, grasses, and bare soil. Parameterization of these different land cover types is derived from the IGBP database (IGBP, 2018).

The subsurface of the study area is heterogeneous in both vertical and horizontal directions. The subsurface of the top 1 m corresponds to three soil layers as defined by the

SSURGO database and then corrected based on the land cover and geologic maps to include the outcropping of the bedrock. Two main types of soil are distinguished within the area: sandy loam and clay loam. The geology of the subsurface between 1 m and 8 m below the ground was defined with USGS maps, which were further improved by local knowledge by Pribulick et al., (2016). This subsurface region is highly heterogeneous with different formations such as crystalline, sedimentary rocks, unconsolidated rocks, alluvial deposits, and debris flow. The bottom layer of the domain (extending from 8 m below the ground surface to the bottom of the model) is assumed homogeneous and represents the fractured bedrock.

We simulated the water year (WY) 2015, a relatively average WY in the region based on average precipitation and temperature patterns. The meteorological forcing of the model has a resolution of an hour and is derived from two gridded datasets: PRISM and NLDAS. The PRISM dataset (Daly et al., 2008) is used for precipitation and temperature because of their accuracy and high spatial resolution (800m). However, the daily resolution of PRISM impedes its ability to be used to reproduce diurnal cycles, an important factor when studying land surface processes requiring hourly forcing. The phase 2 of the North America Land Data Assimilation System NLDAS-2 forcing (Cosgrove et al., 2003) on the contrary provides hourly changes in precipitation and temperature yet are only available at coarser, 1/8 degree, resolutions. As such, we employ a mass-conservative temporal interpolation, which disaggregates the total daily PRISM precipitation into an hourly time series based on the signal of the NLDAS-2 precipitation and temperature trends. For the other forcing variables (i.e. shortwave and longwave radiation, wind speed, atmospheric pressure, and specific humidity), we use NLDAS-2 forcing, (Cosgrove et al., 2003).

3. Results and discussions

3.1. Hillslope functional zonation

As shown in Figure 1b, 127 hillslopes are delineated in the East River watershed based on the elevation following (Noël et al., 2014) and using Topotoolbox developed by (Schwanghart & Scherler, 2014). A threshold of flow accumulation was set to match the stream observations at major tributaries of the East River (Carroll et al., 2018). Because the hillslope delineation could be sensitive to the threshold of the drainage area, we tested different threshold values to find that the selected threshold value represents the scale of hillslope at which the within-hillslope variability of key properties (such as elevation and aspect) is minimized and hillslope-averaged properties can account for the majority of watershed-scale variability (Wainwright et al., 2021). Figure 2 shows the temporal variations of SWE and water table depth at a selected hillslope (see its location in Figure 1) in the watershed. All hydrologic variables have been computed at a hillslope scale by computing the arithmetic average of all cells in each hillslope. In this mountainous watershed, where the largest changes in groundwater are mostly a result of snowmelt, groundwater decreases from the beginning of the WY (i.e. October) to the beginning of snowmelt (i.e. May) period. As the snow starts to melt, groundwater levels start to raise. The peak discharge is mostly observed in June and July when the snow melts over shallow water tables. This period also corresponds to the period of high ET, as both the evaporative demand and the water availability are high. To characterize these groundwater dynamics, we define two variables:

- ΔP_1 represents the changes in groundwater levels between the initial and the minimum groundwater levels during the baseflow conditions. This variable indicates the ability of the hillslope to release water.

https://doi.org/10.5194/hess-2021-520
Preprint. Discussion started: 26 October 2021

Hydrology and Earth System Sciences
Open Access
EGU
Discussions

- ΔP_2 quantifies the changes in groundwater levels between the peak flow (i.e. the period with the shallowest water table depth) and the baseflow conditions and hence contains information about the storage and the recharge capacity of the hillslope.

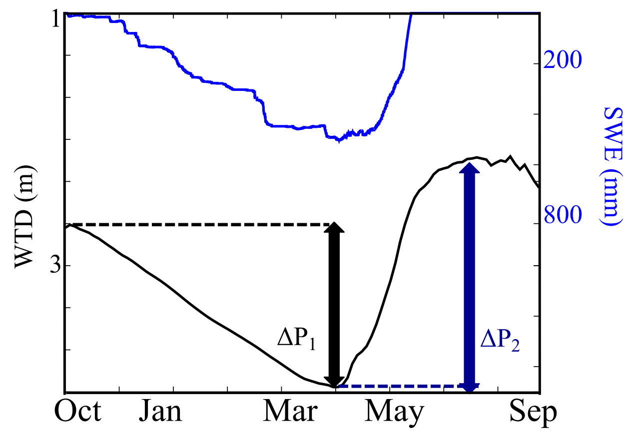

Figure 2: Temporal variations of water table depth (WTD) and SWE at an example hillslope. The location of the hillslope is shown in Figure 1.

These two key variables define the ability of the hillslope to recharge, store, and release water, a key "hydrologic function". The ability of a hillslope to release water as described by ΔP_1 mainly depends on ET and discharge while the recharge quantified by ΔP_2 is mostly a function of precipitation and later on snowmelt in this mountainous watershed.

Figure 3 shows the classification of some key processes controlling the releases and recharges of water at a hillslope scale: temperature, precipitation, SWE, and ET. As expected, the hillslopes characterized by high SWE have high precipitation rates and low temperatures in contrast to the hillslopes with low SWE. However, ET shows a different pattern, because it depends on both water availability but also the ET demands, which depends on the type of land cover.

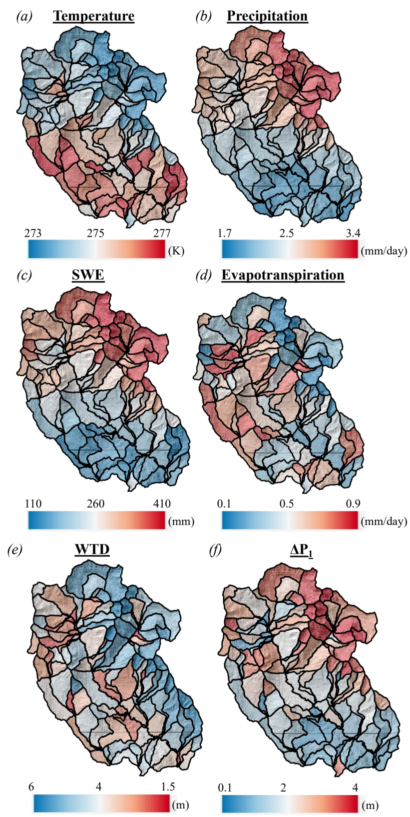

Figure 3: Spatial distributions of hillslope annual average values of (a) temperature, (b) precipitation, (c) snow water equivalent (SWE), (d) evapotranspiration, (e) water table depth (WTD) and (e) seasonal changes in groundwater levels ΔP_1

The spatial variability in ΔP_1 and annual average Water Table Depth (WTD) across different hillslopes are also depicted in Figure 3. These two patterns are different from each other, and they are also different from the ones associated with the land surface processes which eventually control the recharge and release of water (SWE and ET). Nevertheless, the spatial distributions of WTD and ΔP_1 provide complementary information, with areas with high ΔP_1 having low WTD because the strong changes in groundwater levels, as quantified by ΔP_1, lead to a deep WTD. We also note that the variabilities of these variables within hillslopes are smaller than the ones across hillslopes, which is consistent with Wainwright et al. (2021).

To better understand the relationship between ΔP_1 and the factors controlling the recharge and release of water at a hillslope scale, we study the Pearson correlation coefficient between ΔP_1 and the elevation, the percent of the dominant land cover, TWI, AI, ET, SWE, and WTD (Figure 4).

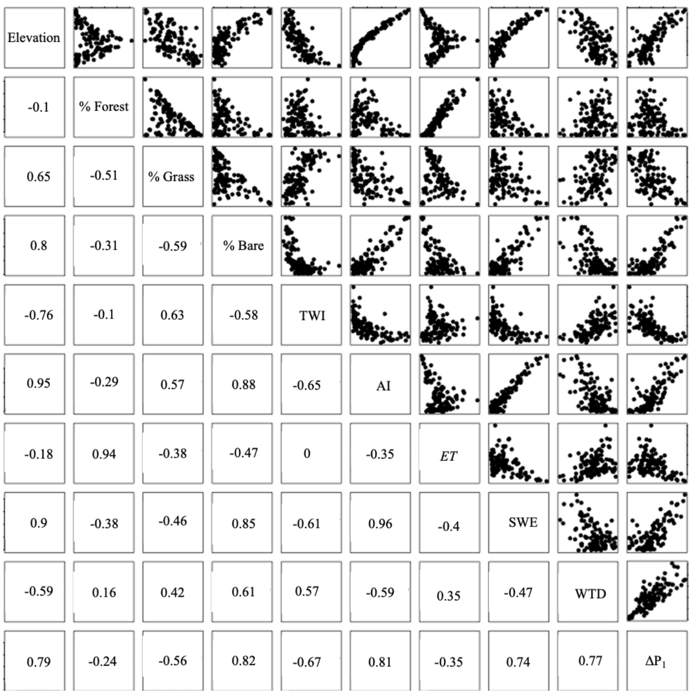

Figure 4: Pearson's correlations between the selected variables for hillslope similarity classifications: elevation, percent of the main land cover type (forest, grassland, and bare soil), topographic wetness index (TWI), aridity index (AI), evapotranspiration (ET), snow water equivalent (SWE), water table depth (WTD), and seasonal changes in groundwater ΔP_1.

https://doi.org/10.5194/hess-2021-520
Preprint. Discussion started: 26 October 2021

Results for ΔP_2 are not shown because it is strongly correlated to ΔP_1 and the two variables provide the same information. TWI, AI, SWE, WTD, and ΔP_1 are significantly correlated with elevation. In particular, elevation has a dominant control on AI and SWE with a correlation coefficient higher than 0.9. We observe nonlinearity such that TWI increases in the lower elevation and that AI becomes constant at the lower elevation. The percentage of forest cover has a quadratic relationship with elevation. A high correlation between the percent of forests and the elevation is found in the mid-elevation whereas grassland shows a high correlation in low and high elevations. ET is well correlated to the percent of forests, where hillslopes with high ET have a high percent of forests. ΔP_1 is, in general, well correlated to all these variables; it, therefore, indicates that the selected variable contains valuable information about these variables. Specifically, ΔP_1 shows a high correlation with SWE, elevation, AI, and WTD with a Pearson correlation coefficient greater than 0.7. Changes in groundwater levels in this mountainous watershed are mostly controlled by the snow dynamics. The two variables with low correlations with ΔP_1 are the ET and the percent of forests. ET is related to groundwater dynamics in a nonlinear way (Condon et al., 2013; Ferguson & Maxwell, 2010; Rahman et al., 2016). Regions with shallow WTDs have the highest ET fluxes and this flux typically decreases exponentially with the depth, where after a certain threshold a disconnection between the groundwater and the atmosphere occurs, and changes in WTD do not impact ET.

We examine eight different hillslope classifications using the variables listed below. For each method, three functional zones are delineated (see Figure 5). Except for the clustering approaches, grouping was made based on the manual selection of natural grouping in the probability density function.

https://doi.org/10.5194/hess-2021-520
Preprint. Discussion started: 26 October 2021

Hydrology and Earth System Sciences
Discussions
Open Access

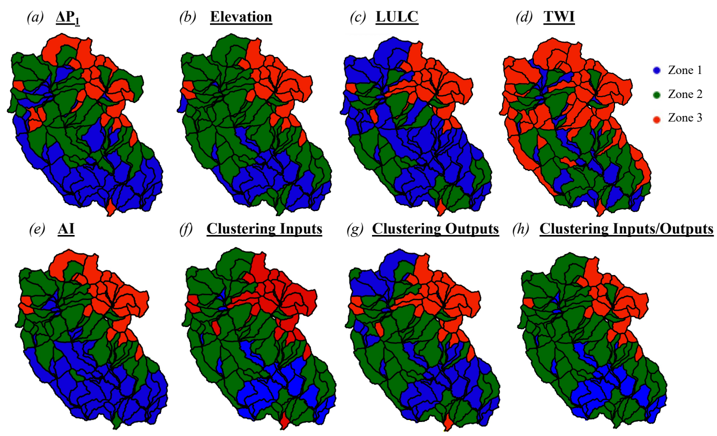

Figure 5: Hillslope zonations based on (a) ΔP_1, (b) elevation, (c) land cover (LULC), (d) topographic wetness index (TWI), (e) aridity index (AI), and clustering with (f) inputs, (g) outputs, and (h) inputs and outputs variables.

- ΔP_1: a preliminary analysis of the seasonal changes in groundwater levels allows distinguishing three main hillslope categories with similar ΔP_1. Zone 1 comprises hillslopes whose ΔP_1 are less than 1.5 m, ΔP_1 of hillslopes of zone 2 are comprised between 1.5 m and 2.5 m, and Zone 3 group all hillslopes with ΔP_1 greater than 2.5 m.
- Elevation: in mountainous watersheds, because the differences in hydroclimate are primarily driven by elevation, hillslopes with similar elevations will potentially have similar land surface signatures. Using elevation, we define three zones, characterizing low (Zone 1, average hillslope elevation less than 3000 m), mid (Zone 2, average hillslope elevation comprises between 3000 m and 3500 m), and high elevation (Zone 3, hillslope with an average elevation greater than 3500 m).

- Land cover and land use (LULC): hillslopes can also be classified based on their dominant land cover. Land cover shapes land surface processes, which in turn affect subsurface dynamics and the water balance at the hillslope scale. In this study, we define three different types of hillslopes based on their dominant land cover: Zone 1 describes hillslopes that have predominantly grasses as land cover, Zone 2 for hillslopes with more than 50% of forest, and Zone 3 for hillslopes where bare soil is the dominant land cover.
- TWI: The Topographic Wetness index commonly used to classify hillslopes is given by: $ln\,(\frac{\alpha}{tan(\beta)})$. Where α is the upslope draining area and β the local angle. We define 3 zones with high (TWI>1, Zone 1), mid (TWI comprises between 1 and 0.2 Zone 2), and low (TWI<0.2, Zone 3) TWI.
- Aridity index (AI): the AI (ETP/Precipitation, where ETP is the potential evapotranspiration) represents the ratio of the average demand for moisture to the average supply of moisture. We derive the spatial distribution of the aridity index in the East River from the Global Aridity Index dataset (CGIAR-CSI, 2019). We then define three zones. Zone 1 comprises hillslopes with AI less than 0.45, Zone 2 describes hillslopes with AI between 0.45 and 0.55, and hillslopes of Zone 3 have an AI greater than 0.55.
- Clustering: we define the hillslope similarity based on clustering of ParFlow-CLM input and output data layers. Clustering was performed in three different ways, using the following data: (1) model input (elevation, percentage of the main land cover type, TWI, and AI), referred to hereafter as the "clustering input" (C.I.) method, (2) model output (ET, SWE, WTD, and ΔP1), referred to hereafter as the

https://doi.org/10.5194/hess-2021-520
Preprint. Discussion started: 26 October 2021

"clustering output" (C.O.) method, and (3) both model input and output data layers, referred to hereafter as the "clustering input-output" (C.I.O.) method. We use hierarchical clustering, which is a decision-tree-based method that divides data points based on a series of binary splits (Devadoss et al., 2020; Kassambara, 2017). We define the linkage (or the distance) between any two clusters based on the Euclidian distance and the Ward method that computes the variance within each cluster, measuring the distance between each observation and the cluster's mean, and then taking the sum of the distances' squares.

3.2. Comparisons

To test the ability of the eight selected classifications to identify and categorize hillslopes with similar static characteristics and hydrologic functions, we assess each method's ability to describe several characteristics of the hillslope. These include a spectrum of datasets varying from those which are widely available (e.g. LULC and elevation) to those which are time-variant (e.g. hydroclimatic data such as temperature and precipitation), and modeled descriptions (e.g. water and energy fluxes). For each variable, zone, and classification scheme, we compute the mean (μ) of the hillslope values and the corresponding coefficient of variation (CV), see Table 1. We also calculate the mean of the CV of the different zones for each variable and classification scheme. This allows us to determine the classification scheme that categorizes zones with the least variability, an important metric that provides a degree of performance for the method's ability to delineate zones.

https://doi.org/10.5194/hess-2021-520
Preprint. Discussion started: 26 October 2021

Variable: Elevation

	ΔP_1	Elevation	LULC	TWI
Zone 1	μ=3027 ; CV=0.25	μ=2884 ; CV=0.02	μ=3099 ; CV=0.06	μ=2853 ; CV=0.25
Zone 2	μ=3226 ; CV=0.06	μ=3233 ; CV=0.06	μ=3065 ; CV=0.16	μ=2637 ; CV=0.41
Zone 3	μ=3593 ; CV=0.04	μ=3641 ; CV=0.04	μ=3595 ; CV=0.04	μ=1999 ; CV=0.84

	AI	Clustering Input	Clustering Output	Clustering I. O.
Zone 1	μ=2947 ; CV=0.03	μ=3202 ; CV=0.04	μ=3029 ; CV=0.07	μ=3232 ; CV=0.049
Zone 2	μ=3285 ; CV=0.03	μ=2903 ; CV=0.03	μ=3175 ; CV=0.04	μ=2904 ; CV=0.034
Zone 3	μ=3625 ; CV=0.03	μ=3592 ; CV=0.03	μ=3605 ; CV=0.03	μ=3658 ; CV=0.025

Variable: Precipitation

	ΔP_1	Elevation	LULC	TWI
Zone 1	μ=2.24 ; CV=0.21	μ=2.11 ; CV=0.22	μ=2.42 ; CV=0.22	μ=2.38 ; CV=0.23
Zone 2	μ=2.68 ; CV=0.18	μ=2.77 ; CV=0.22	μ=2.39 ; CV=0.20	μ=2.37 ; CV=0.22
Zone 3	μ=3.26 ; CV=0.15	μ=3.55 ; CV=0.09	μ=3.26 ; CV=0.16	μ=2.74 ; CV=0.23

	AI	Clustering Input	Clustering Output	Clustering I. O.
Zone 1	μ=2.10 ; CV=0.15	μ=2.68 ; CV=0.18	μ=2.33 ; CV=0.22	μ=2.73 ; CV=0.18
Zone 2	μ=2.74 ; CV=0.17	μ=2.06 ; CV=0.16	μ=2.63 ; CV=0.18	μ=2.07 ; CV=0.17
Zone 3	μ=3.39 ; CV=0.12	μ=3.41 ; CV=0.11	μ=3.43 ; CV=0.11	μ=3.56 ; CV=0.06

Variable: Temperature

	ΔP_1	Elevation	LULC	TWI
Zone 1	μ=276.5 ; CV=0.001	μ=276.2 ; CV=0.003	μ=276.1 ; CV=0.002	μ=276.3 ; CV=0.001
Zone 2	μ=275.9 ; CV=0.002	μ=276.0 ; CV=0.003	μ=276.4 ; CV=0.001	μ=276.2 ; CV=0.002
Zone 3	μ=274.5 ; CV=0.002	μ=274.1 ; CV=0.002	μ=274.4 ; CV=0.002	μ=275.6 ; CV=0.003

	AI	Clustering Input	Clustering Output	Clustering I. O.
Zone 1	μ=276.6 ; CV=0.001	μ=276.2 ; CV=0.002	μ=276.2 ; CV=0.002	μ=276.1 ; CV=0.002
Zone 2	μ=275.8 ; CV=0.002	μ=276.5 ; CV=0.001	μ=276.3 ; CV=0.002	μ=276.5 ; CV=0.001
Zone 3	μ=274.3 ; CV=0.002	μ=274.4 ; CV=0.003	μ=274.3 ; CV=0.002	μ=274.1 ; CV=0.002

Variable: SWE

	ΔP_1	Elevation	LULC	TWI
Zone 1	μ=152 ; CV=0.30	μ=149 ; CV=0.38	μ=181 ; CV=0.34	μ=169 ; CV=0.50
Zone 2	μ=204 ; CV=0.34	μ=201 ; CV=0.43	μ=151 ; CV=0.29	μ=165 ; CV=0.39
Zone 3	μ=335 ; CV=0.31	μ=389 ; CV=0.26	μ=339 ; CV=0.29	μ=234 ; CV=0.46

	AI	Clustering Input	Clustering Output	Clustering I. O.
Zone 1	μ=137 ; CV=0.18	μ=191 ; CV=0.32	μ=173 ; CV=0.34	μ=200 ; CV=0.33
Zone 2	μ=206 ; CV=0.25	μ=145 ; CV=0.17	μ=179 ; CV=0.30	μ=146 ; CV=0.20
Zone 3	μ=360 ; CV=0.24	μ=359 ; CV=0.25	μ=365 ; CV=0.23	μ=396 ; CV=0.18

Variable: ET

ΔP_1	Elevation	LULC	TWI
Zone 1: μ=0.42 ; CV=0.47	Zone 1: μ=0.35 ; CV=0.75	Zone 1: μ=0.31 ; CV=0.36	Zone 1: μ=0.37 ; CV=0.58
Zone 2: μ=0.41 ; CV=0.47	Zone 2: μ=0.48 ; CV=0.54	Zone 2: μ=0.61 ; CV=0.27	Zone 2: μ=0.41 ; CV=0.49
Zone 3: μ=0.17 ; CV=0.74	Zone 3: μ=0.15 ; CV=0.90	Zone 3: μ=0.19 ; CV=0.69	Zone 3: μ=0.35 ; CV=0.56
AI	**Clustering Input**	**Clustering Output**	**Clustering I. O.**
Zone 1: μ=0.40 ; CV=0.46	Zone 1: μ=0.49 ; CV=0.37	Zone 1: μ=0.27 ; CV=0.29	Zone 1: μ=0.48 ; CV=0.38
Zone 2: μ=0.45 ; CV=0.45	Zone 2: μ=0.25 ; CV=0.32	Zone 2: μ=0.55 ; CV=0.29	Zone 2: μ=0.25 ; CV=0.31
Zone 3: μ=0.14 ; CV=0.58	Zone 3: μ=0.19 ; CV=0.68	Zone 3: μ=0.18 ; CV=0.65	Zone 3: μ=0.12 ; CV=0.57

Variable: Saturation

ΔP_1	Elevation	LULC	TWI
Zone 1: μ=0.77 ; CV=0.14	Zone 1: μ=0.75 ; CV=0.23	Zone 1: μ=0.75 ; CV=0.14	Zone 1: μ=0.81 ; CV=0.14
Zone 2: μ=0.69 ; CV=0.10	Zone 2: μ=0.73 ; CV=0.16	Zone 2: μ=0.71 ; CV=0.15	Zone 2: μ=0.72 ; CV=0.12
Zone 3: μ=0.66 ; CV=0.11	Zone 3: μ=0.67 ; CV=0.13	Zone 3: μ=0.68 ; CV=0.09	Zone 3: μ=0.70 ; CV=0.13
AI	**Clustering Input**	**Clustering Output**	**Clustering I. O.**
Zone 1: μ=0.75 ; CV=0.15	Zone 1: μ=0.72 ; CV=0.11	Zone 1: μ=0.76 ; CV=0.15	Zone 1: μ=0.72 ; CV=0.10
Zone 2: μ=0.73 ; CV=0.13	Zone 2: μ=0.77 ; CV=0.16	Zone 2: μ=0.72 ; CV=0.10	Zone 2: μ=0.78 ; CV=0.15
Zone 3: μ=0.68 ; CV=0.11	Zone 3: μ=0.69 ; CV=0.09	Zone 3: μ=0.68 ; CV=0.09	Zone 3: μ=0.66 ; CV=0.08

Variable: WTD

ΔP_1	Elevation	LULC	TWI
Zone 1: μ=2.9 ; CV=0.06	Zone 1: μ=3.4 ; CV=0.1	Zone 1: μ=3.0 ; CV=0.06	Zone 1: μ=2.4 ; CV=0.04
Zone 2: μ=3.7 ; CV=0.05	Zone 2: μ=3.2 ; CV=0.07	Zone 2: μ=3.5 ; CV=0.07	Zone 2: μ=3.3 ; CV=0.04
Zone 3: μ=4.8 ; CV=0.07	Zone 3: μ=4.6 ; CV=0.08	Zone 3: μ=4.7 ; CV=0.07	Zone 3: μ=4.0 ; CV=0.1
AI	**Clustering Input**	**Clustering Output**	**Clustering I. O.**
Zone 1: μ=3.1 ; CV=0.06	Zone 1: μ=3.2 ; CV=0.04	Zone 1: μ=2.8 ; CV=0.05	Zone 1: μ=3.3 ; CV=0.04
Zone 2: μ=3.5 ; CV=0.07	Zone 2: μ=2.6 ; CV=0.04	Zone 2: μ=3.2 ; CV=0.04	Zone 2: μ=2.5 ; CV=0.04
Zone 3: μ=4.7 ; CV=0.08	Zone 3: μ=4.4 ; CV=0.06	Zone 3: μ=4.5 ; CV=0.05	Zone 3: μ=4.8 ; CV=0.05

Variable: ΔP_2

ΔP_1	Elevation	LULC	TWI
Zone 1: μ=2.9 ; CV=0.06	Zone 1: μ=3.4 ; CV=0.1	Zone 1: μ=3.0 ; CV=0.06	Zone 1: μ=2.4 ; CV=0.04
Zone 2: μ=3.7 ; CV=0.05	Zone 2: μ=3.2 ; CV=0.07	Zone 2: μ=3.5 ; CV=0.07	Zone 2: μ=3.3 ; CV=0.04
Zone 3: μ=4.8 ; CV=0.07	Zone 3: μ=4.6 ; CV=0.08	Zone 3: μ=4.7 ; CV=0.07	Zone 3: μ=4.0 ; CV=0.1
AI	**Clustering Input**	**Clustering Output**	**Clustering I. O.**
Zone 1: μ=3.1 ; CV=0.06	Zone 1: μ=3.2 ; CV=0.04	Zone 1: μ=2.8 ; CV=0.05	Zone 1: μ=3.3 ; CV=0.04
Zone 2: μ=3.5 ; CV=0.07	Zone 2: μ=2.6 ; CV=0.04	Zone 2: μ=3.2 ; CV=0.04	Zone 2: μ=2.5 ; CV=0.04
Zone 3: μ=4.7 ; CV=0.08	Zone 3: μ=4.4 ; CV=0.06	Zone 3: μ=4.5 ; CV=0.05	Zone 3: μ=4.8 ; CV=0.05

Table 1: Mean μ and coefficient of variation CV of each variable and zone derived from the 8 classifications.

https://doi.org/10.5194/hess-2021-520
Preprint. Discussion started: 26 October 2021

Hydrology and Earth System Sciences
Open Access
Discussions

3.2.1. Similarities in hillslope structure

Elevation plays an important role in shaping the hydroclimate of a given region especially in mountainous watersheds where it controls snow accumulation, the principal driver of the downstream hydrology. Figure 6 shows the elevation distributions associated with the different zones derived from the 8 classifications.

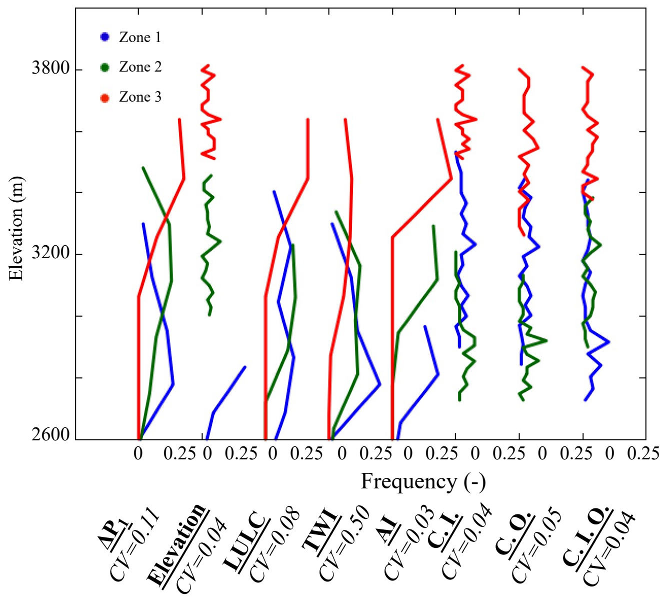

Figure 6: Distributions of hillslope elevation of the three zones derived from ΔP_1, elevation, land cover (LULC), topographic wetness index (TWI), aridity index (AI), and clustering (clustering with inputs C.I., clustering with outputs C.O., and clustering with inputs and outputs C.I.O) hillslope classifications.

By classifying the hillslopes based on their similarity in ΔP_1, we observe that hillslopes with low ΔP have the lowest elevation while the hillslopes of zone 3 (high ΔP_1) have the highest

https://doi.org/10.5194/hess-2021-520
Preprint. Discussion started: 26 October 2021

elevation. Unsurprisingly, the second classification scheme (i.e. elevation-based) clearly distinguishes the hillslopes based on their elevation, as it is the essence of that classification scheme. The AI is also an excellent index for identifying hillslopes with similar elevation as discussed and shown in Figures 4 and 6. The TWI classification performs moderately, where zone 1 and 2 are characterized by similar elevation distributions. Hillslopes with lower TWI are mostly located in high elevation areas on the contrary to the low elevation hillslopes. In the land cover-based classification, most of the grassed hillslopes (zone 1) are in low elevation, forests (zone 2) in mid-elevation, and hillslopes whose landscape is mainly bare soil (zone 3) are in high elevation areas above the tree line. The three clustering classifications allow distinguishing zones with similar elevation, their coefficients of variation are of the same order as the elevation based classification. These three classifications lead to similar results indicating that both inputs and outputs yield the same results.

Table 2 describes the average percentage of the main land cover type at the hillslope scale for each zone and classification. The selected classifications lead to similar conclusions, hillslopes associated with zone 1 have mainly grasses, while hillslopes of zone 2 have mostly identical percentage of forest and grasses in the ΔP1, AI, and elevation classifications. LULC classification allows clearly distinguishing zone 1 (grasses) from zone 2 (hillslopes of these zones have more than 70% of forest). For ΔP_1, elevation, AI, and LULC classifications, zone 3 is mostly comprised of bare soil, as this zone is mostly located in high elevation areas above the tree line. In the TWI classification, zone 1 is characterized by grasses whereas zone 3's land cover located in high elevation with low TWI is bare soil.

https://doi.org/10.5194/hess-2021-520
Preprint. Discussion started: 26 October 2021

Hydrology and Earth System Sciences
Discussions

ΔP_1	**Forest**	**Grassland**	**Bare Soil**
Zone 1	0.35	0.55	0.10
Zone 2	0.35	0.43	0.22
Zone 3	0.11	0.27	0.62
CV	0.97	0.56	0.69
Elevation	**Forest**	**Grassland**	**Bare Soil**
Zone 1	0.28	0.56	0.15
Zone 2	0.41	0.42	0.17
Zone 3	0.07	0.26	0.68
CV	1.33	0.76	1.07
Land Cover	**Forest**	**Grassland**	**Bare Soil**
Zone 1	0.23	0.67	0.14
Zone 2	0.72	0.26	0.12
Zone 3	0.12	0.22	0.66
CV	0.67	0.45	0.64
Topographic Wetness Index (TWI)	**Forest**	**Grasslands**	**Bare Soil**
Zone 1	0.24	0.66	0.10
Zone 2	0.35	0.51	0.14
Zone 3	0.32	0.35	0.33
CV	1.47	0.49	0.95
Aridity Index	**Forest**	**Grassland**	**Bare Soil**
Zone 1	0.34	0.57	0.09
Zone 2	0.37	0.41	0.22
Zone 3	0.07	0.32	0.61
CV	0.91	0.56	0.69
Clustering with input layers	**Forest**	**Grassland**	**Bare Soil**
Zone 1	0.44	0.42	0.14
Zone 2	0.11	0.83	0.06
Zone 3	0.12	0.25	0.63
CV	0.83	0.38	0.62
Clustering with output layers	**Forest**	**Grasslands**	**Bare Soil**
Zone 1	0.14	0.77	0.09
Zone 2	0.52	0.34	0.15
Zone 3	0.11	0.25	0.64
CV	0.77	0.38	0.61

https://doi.org/10.5194/hess-2021-520
Preprint. Discussion started: 26 October 2021

Clustering with inputs and outputs	**Forest**	**Grassland**	**Bare Soil**
Zone 1	0.42	0.40	0.18
Zone 2	0.12	0.82	0.06
Zone 3	0.05	0.24	0.70
CV	0.87	0.41	0.65

Table 2: Average values of hillslope percentage of forests, grasslands, and bare soils for each zone and classification

3.2.2. Similarities in hydroclimate

Figures 7a and b depict the distributions of precipitation and temperature obtained with the eight selected classifications. The classifications based on elevation and AI allows clearly distinguishing the hydroclimate associated with each zone. Zone 1 located in low elevation has low precipitation rates and high temperatures, contrary to zone 3. Zone 2 is characterized by an intermediate climate. Our approach based on seasonal variation in groundwater changes leads to conclusions similar to the clustering and AI based classifications. The resulting average CV of these three types of classifications are similar. These three classifications remain the only methods that allow characterizing each zone by its hydroclimate. Although, we note that in the three clustering classifications as well as in the ΔP approach, Zones 1 and 2 have similar hydroclimate, which is not the case in the AI based classification. While the classification based on the land cover clearly identifies the typical hydroclimate of the hillslopes of zone 3 (bare soil), the two remaining zones have the same hydroclimate. The classification based on the TWI does not regroup hillslopes based on their hydroclimates; again this type of classification mainly describes how a given hillslope release water based on its topographic structure. Nevertheless, it is important to account for the hydroclimate of hillslopes in a classification.

https://doi.org/10.5194/hess-2021-520
Preprint. Discussion started: 26 October 2021

Hydrology and Earth System Sciences
Discussions
Open Access

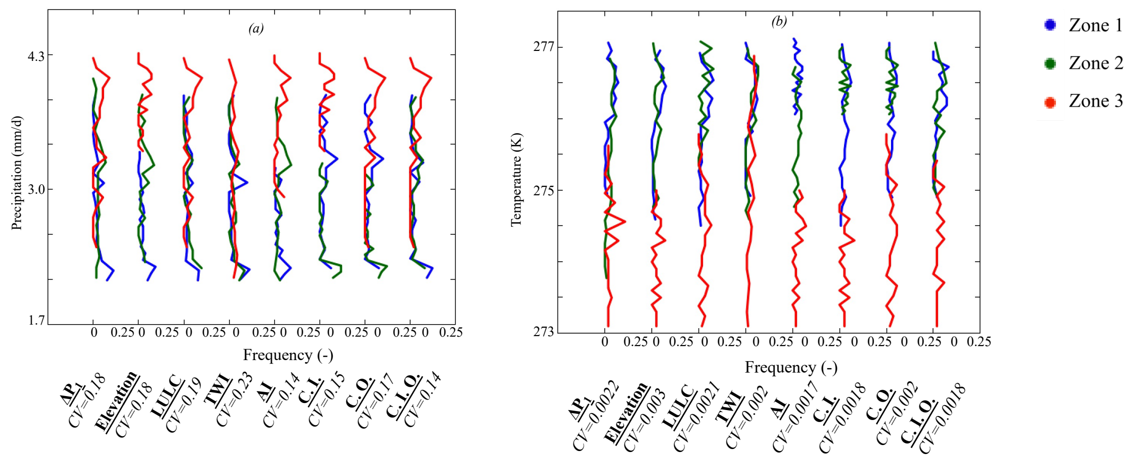

Figure 7: Distributions of hillslope (a) annual average daily rates of precipitation and (b) annual average temperature of the three zones derived from ΔP_1, elevation, land cover (LULC), topographic wetness index (TWI), aridity index (AI), and clustering (clustering with inputs C.I., clustering with outputs C.O., and clustering with inputs and outputs C.I.O) hillslope classifications.

3.2.3. Similarities in hydrologic function

A hillslope hydrologic function should aim to describe how a hillslope partitions, stores, retains, and releases water. Many hydrologic processes, both at the land surface and in the subsurface, are simultaneously occurring, which typically result in non-linear dynamics. In this section, we show the performance of the classification schemes to delineate regions exhibiting different surface and subsurface hydrologic behavior.

3.2.3.1. Land surface processes

https://doi.org/10.5194/hess-2021-520
Preprint. Discussion started: 26 October 2021

A robust classification of hillslopes in mountainous watersheds should integrate the similarity in snow dynamics. Figure 8a illustrates the SWE distribution associated with each zone and classification. Because SWE dynamics are primarily driven by elevation and the precipitation, the classifications based on the AI and clustering have the lowest average of the CV followed by the land cover and the ΔP_1 based classification. The land cover spatial distribution contains information about elevation especially in high elevation areas where some hillslopes are located above the tree line. The ΔP_1 approach accounts for SWE dynamics because the seasonal changes in groundwater depend on the snowmelt, ΔP_1 is highly correlated to SWE as discussed in section 3.1.

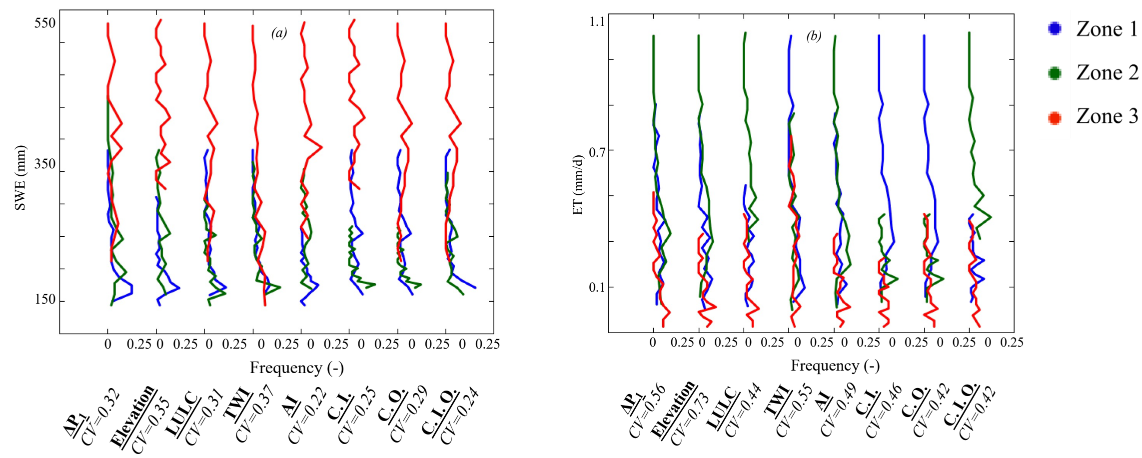

Figure 8: Distributions of hillslope land surface variables (a) annual average SWE and (b) annual average daily rates of ET of the three zones derived from ΔP_1, elevation, land cover (LULC), topographic wetness index (TWI), aridity index (AI), and clustering (clustering with inputs C.I., clustering with outputs C.O., and clustering with inputs and outputs C.I.O) hillslope classifications.

https://doi.org/10.5194/hess-2021-520
Preprint. Discussion started: 26 October 2021

The spatial distribution of ET is controlled by many factors, including soil moisture, land cover, and subsurface flow. As a result, the land cover based classification performs well at delineating hillslopes with similar ET rates (Figure 8b). Consistent with the aforementioned results, the other classification schemes performing well are the ones based on clustering, followed by the AI based classification. To some extent, the TWI and elevation classifications poorly distinguish hillslopes with similar ET. The average CV associated with the ΔP_1 classification is close to that of the classifications based on land cover and AI. As stated in many studies (Ferguson & Maxwell, 2010; Maina & Siirila-Woodburn, 2020), subsurface flow affects ET, as such information about subsurface flow contains valuable information about the ET even if the correlation between ΔP_1 and ET is nonlinear.

3.2.3.2. Similarities in subsurface flow

We investigate the ability of the eight selected classifications to identify hillslopes with similar subsurface hydrodynamics. We study the average saturation of the first 10 cm of the soil throughout the WY, the yearly average of water table depth, and the seasonal changes in groundwater levels ΔP_2. Soil saturation is a key feature in both subsurface and atmospheric dynamics; it controls ET and groundwater recharge. Therefore, an appropriate hillslope classification should be able to identify and categorize hillslope with similar soil moisture patterns. The averages of the CV associated with the classifications based on ΔP_1, TWI, AI, land cover, and clustering are very similar (Figure 9a). As the land cover based classification adequately regroups hillslopes with similar ET, it also allows regrouping hillslopes with similar soil saturation. Because the TWI approach describes water transfer, it serves as a good indicator of soil saturation like the AI. Similar to the results above, the clustering based approaches

https://doi.org/10.5194/hess-2021-520
Preprint. Discussion started: 26 October 2021

perform well in the classification of hillslopes based on their similarity in saturation. The ΔP_1 based classification has one of the lowest averages of CV due to the strong connection between the changes in groundwater and soil saturation. Elevation based classification fails to identify hillslope with similar soil saturation, where the distributions of the three defined zones show overlap.

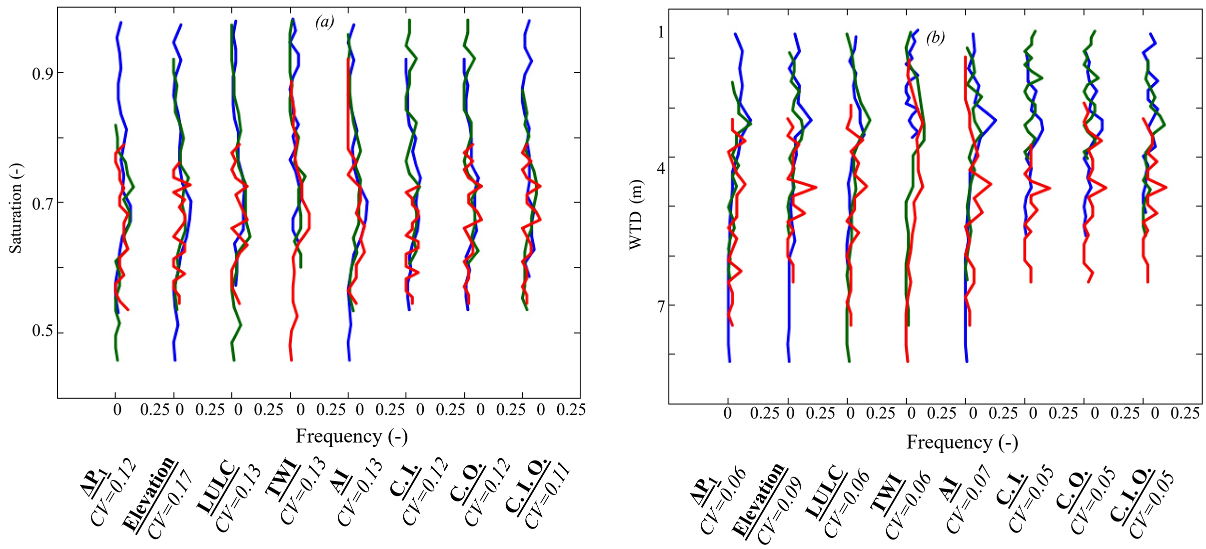

https://doi.org/10.5194/hess-2021-520
Preprint. Discussion started: 26 October 2021

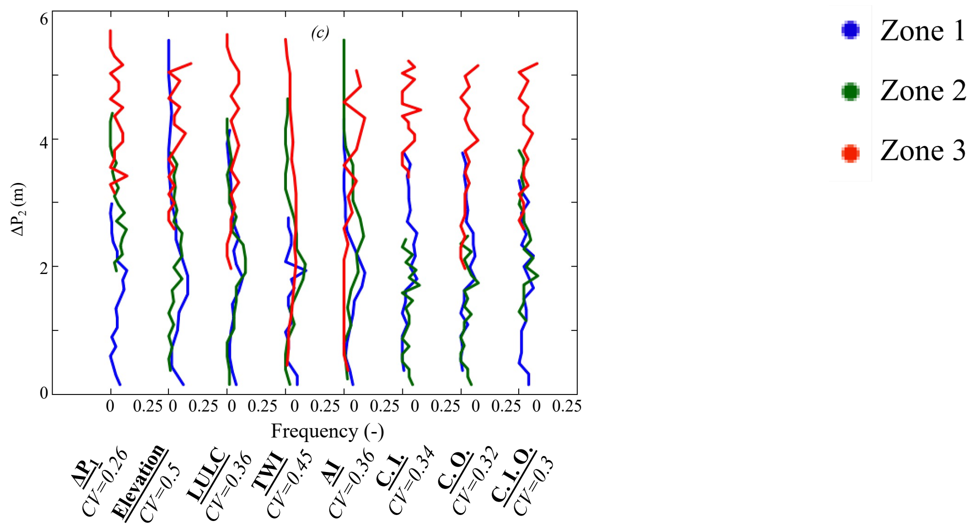

Figure 9: Distributions of hillslope (a) saturation, (b) WTD, and ΔP_2 of the three zones derived from ΔP_1, elevation, land cover (LULC), topographic wetness index (TWI), aridity index (AI), and clustering (clustering with inputs C.I., clustering with outputs C.O., and clustering with inputs and outputs C.I.O) hillslope classifications.

Groundwater storage is mostly quantified in terms of WTD. WTD is an important variable for determining water storage at a hillslope scale. Here, we quantify the average WTD throughout the year. As expected, the ΔP_1 based classification groups hillslopes with similar WTD (Figure 9b). Zone 1 located in low elevation has the shallowest WTD and the lowest ΔP_1, contrary to zone 3. Zone 2 exhibits an intermediary behavior. The TWI and land cover classification schemes also are good methods for identifying hillslope with similar changes in WTD. Hillslopes with low TWI (Zone 3) have the deepest WTD, contrary to the hillslopes of Zone 1. The land cover based classification indicates that most of the forest (Zone 2) and bare soil (Zone 3) hillslopes have deep WTD whereas grasses (Zone 1) hillslopes have the shallowest

WTD. The elevation-based classification scheme doesn't accurately regroup hillslopes with similar WTD, and its average CV remains higher than the 4 other classification schemes. The AI method, like the elevation method, isn't a good variable for identifying hillslopes with similar WTD. In fact, all the three zones overlap in terms of WTD even if their AIs are distinct. Results from the clustering approach are similar to the ΔP_1 based classification with a CV of the same order, yet there isn't a clear distinction between Zone 1 and 2 in these approaches.

Figure 9c illustrates the distributions of the seasonal changes in groundwater levels for each classification and zone. The classification based on ΔP_1 groups hillslopes with similar ΔP_2 as expected. Another suitable approach to group hillslopes with similar ΔP_2 is the land cover classification. Zone 3 characterizing bare soil hillslopes has the highest $\Delta P_{2,}$ unlike zones 1 and 2. The AI classification shows that the majority of zone 3 hillslopes have high ΔP_2 whereas zone 2 hillslopes have low $\Delta P_{2,}$ followed by zone 1 hillslopes. In terms of ΔP_2 similarity, the elevation-based classification outperforms the TWI. The clustering approaches area good way of grouping with hillslopes with similar ΔP_2 especially the clustering approach based on inputs variables CI. The two other clustering approaches (outputs and inputs and outputs) do not distinguish zone 1 from zone 2.

3.2.4. Advantages of a similarity index based ΔP

Depending on the purpose of the identification of similar hillslopes, the appropriate classification scheme may change. Nonetheless, it is important for any classification to identify hillslopes with similar hydrologic functions. As demonstrated here, the advantage of using ΔP_1 to identify similar hillslopes is that many hydrologic processes are embedded in the seasonal changes in groundwater. Our comparisons have shown that by using a ΔP_1 classification scheme to identify hillslopes of similar nature, one is able to group regions based on not only similar subsurface hydrodynamics but also similar land surface dynamics. Because these processes are intimately linked to the structure, the static characteristics, and the physical properties of the hillslope, its hydroclimate, and its land cover, the ΔP_1 approach also allows for the identification of hillslopes with similar topographic structures, land cover, and hydroclimates. For these reasons, ΔP_1 could be considered as an integrated variable for hillslope similarity that does not solely depend on a particular hydrologic process or hillslope characteristics.

We, however, highlight that other classifications may outperform the ΔP_1 when looking at a single process or a single characteristic. For instance, our results show that the elevation and AI classifications may be excellent approaches to group hillslopes with similar hydroclimates and snow dynamics. The land cover based classification allows for better identification of hillslopes with similar land surface processes such as ET and soil saturation. Lastly, the TWI classification scheme allows the grouping of hillslopes with similar groundwater dynamics and soil saturation values as it describes the water transfer. In terms of overall performance, our results show that for the study site considered here, the clustering approach is also a very good approach for hillslope classification.

3.2.5. Similarities in hydrologic responses to wet and dry conditions

According to McDonnell & Woods, (2004) and Wagener et al., (2007), any classification should be able to predict the dynamics of the hillslopes. We test the ability of the ΔP_1 based classification to predict the dynamics of the hillslopes in wet and dry conditions. A possible limitation of a classification based on a hydrologic process is that the latter may be linked to the conditions of the selected year. Hydrologic responses are by essence nonlinear and may strongly

https://doi.org/10.5194/hess-2021-520
Preprint. Discussion started: 26 October 2021

change from year to year. In addition, compared to the intrinsic characteristics of the hillslope (elevation, topographic index, and land cover), which are only variable if long periods of time are considered; the scale at which hydrologic processes change is much shorter. Therefore, a classification scheme based on a process-based approach may be time-dependent. We previously quantified ΔP_1 using the seasonal changes in groundwater in an average WY. In this section, we compare the response of each zone to dry and wet conditions. We extend our simulation from the WY 2015 to include the WYs 2016, 2017, and 2018, then we analyze WYs 2017 and 2018. This 4-year simulation covers a relatively wet (2017) and dry (2018) WY. The annual average precipitation in 2017 was ~15% higher than the annual average precipitation in 2015. After this wet WY, the watershed is characterized by a dry climate in 2018, with average precipitation almost 50% below the normal conditions. Figure 10 shows the distributions of hillslope annual average values of precipitation and ET, and the hillslope ΔP_2 associated with the defined ΔP_1 zones and for both the wet WY 2017 and the dry WY 2018. We have selected the key variables describing the hydroclimate (Precipitation), land surface processes (ET), and subsurface hydrodynamics (ΔP_2).

https://doi.org/10.5194/hess-2021-520
Preprint. Discussion started: 26 October 2021

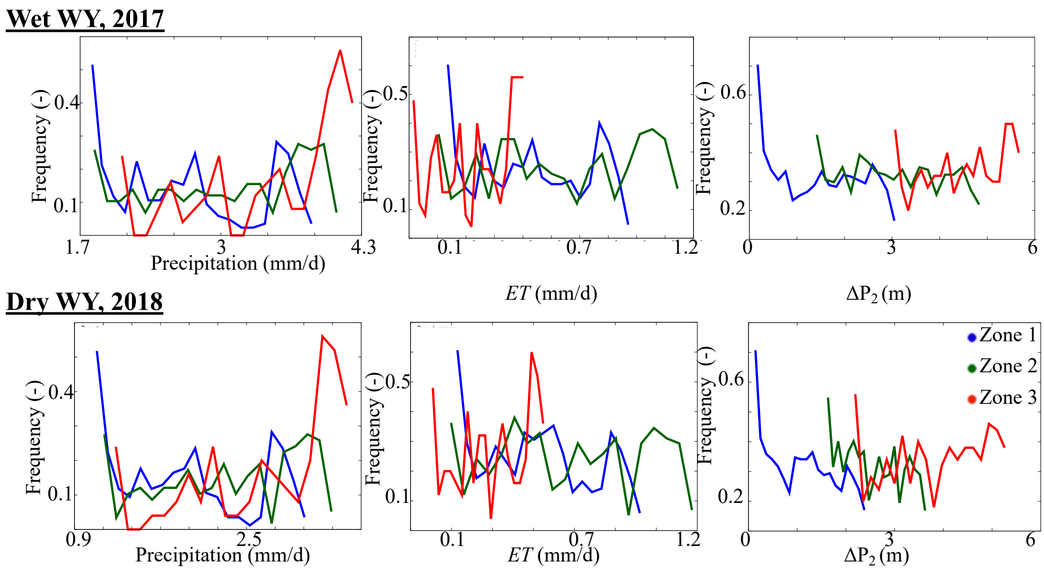

Figure 10: Distributions of hillslope annual average daily rates of precipitation and evapotranspiration (ET), and the hillslope seasonal changes in groundwater levels (ΔP_2) in 2017 (wet WY) and 2018 (dry WY) of the three zones derived from the WY 2015 ΔP_1

At first glance, for both dry and wet years and selected processes, all zones remain distinct. Zone 1 regrouping hillslopes with low seasonal changes in groundwater located in low elevation remains with low precipitation, high ET, and low seasonal changes in groundwater through both wet and dry years. Zone 3 describing hillslopes with high seasonal changes in groundwater has the highest precipitation in the area during both the wet and dry years. Hillslopes of zone 2, located in mid-elevation, have most of their hydrologic dynamics in between those of zone 1 and 3 except their ET, which is the highest in the area due to the presence of forest. Our results show that although we defined hillslopes classification based on a hydrologic process during an average WY, our classification can predict the similarity of the dynamics of these hillslopes in wet and dry conditions. The ΔP_1 based classification approach is, therefore, robust in predicting similarity in hydrologic responses under both wet and dry conditions.

4. Summary and conclusions

In this study, we use the seasonal changes in groundwater levels, termed ΔP_1 (see definition in Figure 2), to identify and categorize similar hillslopes. The seasonal change in groundwater is an important and unique variable as many hydrologic processes including land surface processes and hydroclimatic effects propagate to affect this variable. Our results show that the ΔP_1 classification allows transcending the uniqueness of place inherent in traditional classifications. We defined three zones based on their similarity in ΔP_1. For a test case site in the East River watershed, zone 1 characterizes hillslopes with low ΔP_1; these hillslopes are mostly located in low elevation areas, their main land cover is grassland, and their ET is high because their WTDs are shallow. Zone 3, on the opposite of zone 1 is located in high elevation areas and has high ΔP_1; the hydroclimate leads to high snow accumulation and low ET. Hillslopes of zone 3 are mostly bare soil. Zone 2 is in-between these two zones, most of the hillslopes of this zone are covered by forests.

We tested the ability of the proposed ΔP_1 based classification to identify and group hillslopes with similar static characteristics and hydrologic processes by comparing it with other existing approaches based on elevation, land cover, aridity index, a topographic wetting index, and three clusterings which uses multiple data layers, including model inputs and outputs. Our results show that the ΔP_1 based classification is robust, as it reasonably identifies and categorizes hillslopes with similar elevation, land cover, hydroclimate characteristics, land surface processes (ET and SWE), and subsurface hydrodynamics (water table depths, soil moisture, and seasonal

https://doi.org/10.5194/hess-2021-520
Preprint. Discussion started: 26 October 2021

Hydrology and Earth System Sciences Discussions

changes in water table fluctuations). In general, the other approaches are good in identifying similarity in a single characteristic, a characteristic that is related to the selected variable which determines the classification scheme. Our work also demonstrates that a clustering approach, either based on top-down (inputs) or bottom-up (outputs) performs well. Nevertheless, these approaches like the ΔP_1 based classification, require multiple datasets, each one with its own associated uncertainty. We further demonstrate the robustness of the proposed ΔP_1 based classification by testing its ability to predict hillslope responses to wet and dry hydrologic conditions. The ΔP_1 values used in this demonstration are derived from a model and could be a limitation for sites where simulated outputs are unavailable, or the spatio-temporal resolution of groundwater observations are limited.

This study demonstrates the need for an integrated variable such as groundwater changes to identify and group similar hillslopes. Future studies could aim to define functional zones based on their seasonal changes in groundwater using sophisticated machine learning approaches or optimization procedures. Our results are limited to one catchment, which has snow-dominated hydrology. Future studies could expand the comparison shown here to other watersheds, to include additional classifications, and for different hydroclimate and durations of time (for example, sub-annual or multi-annual classifications).

Data availability

Data supporting the findings of this study are freely available on ESS-DIVE: https://ess-dive.lbl.gov

Author contribution

The authors contribute equally to this work.

Competing interests

The authors declare that they have no conflict of interest.

Acknowledgements

This material is based on work supported as part of the Watershed Function Scientific Focus Area funded by the U.S. Department of Energy, Office of Science, Office of Biological and Environmental Research under Award no. DE-AC02-05CH11231.

https://doi.org/10.5194/hess-2021-520
Preprint. Discussion started: 26 October 2021

Hydrology and Earth System Sciences
Discussions

References

Andréassian, V., Lerat, J., Le Moine, N., & Perrin, C. (2012). Neighbors: Nature's own hydrological models. *Journal of Hydrology*, *414–415*, 49–58. https://doi.org/10.1016/j.jhydrol.2011.10.007

Aryal, S. K., O'Loughlin, E. M., & Mein, R. G. (2002). A similarity approach to predict landscape saturation in catchments. *Water Resources Research*, *38*(10), 26-1-26–16. https://doi.org/10.1029/2001WR000864

Berghuijs, W. R., Sivapalan, M., Woods, R. A., & Savenije, H. H. G. (2014). Patterns of similarity of seasonal water balances: A window into streamflow variability over a range of time scales. *Water Resources Research*, *50*(7), 5638–5661. https://doi.org/10.1002/2014WR015692

Berne, A., Uijlenhoet, R., & Troch, P. A. (2005). Similarity analysis of subsurface flow response of hillslopes with complex geometry. *Water Resources Research*, *41*(9). https://doi.org/10.1029/2004WR003629

Beven, K. J. (2000). Uniqueness of place and process representations in hydrological modelling. *Hydrology and Earth System Sciences*, *4*(2), 203–213. https://doi.org/10.5194/hess-4-203-2000

BEVEN, K. J., & KIRKBY, M. J. (1979). A physically based, variable contributing area model of basin hydrology / Un modèle à base physique de zone d'appel variable de l'hydrologie du bassin versant. *Hydrological Sciences Bulletin*, *24*(1), 43–69. https://doi.org/10.1080/02626667909491834

Bormann, H. (2010). Towards a hydrologically motivated soil texture classification. *Geoderma*, *157*(3), 142–153. https://doi.org/10.1016/j.geoderma.2010.04.005

Bosch, J. M., & Hewlett, J. D. (1982). A review of catchment experiments to determine the effect of vegetation changes on water yield and evapotranspiration. *Journal of Hydrology*, *55*(1), 3–23. https://doi.org/10.1016/0022-1694(82)90117-2

Brown, A. E., Zhang, L., McMahon, T. A., Western, A. W., & Vertessy, R. A. (2005). A review of paired catchment studies for determining changes in water yield resulting from alterations in vegetation. *Journal of Hydrology*, *310*(1), 28–61. https://doi.org/10.1016/j.jhydrol.2004.12.010

Brunner, P., & Simmons, C. T. (2012). HydroGeoSphere: A Fully Integrated, Physically Based Hydrological Model. *Groundwater*, *50*(2), 170–176. https://doi.org/10.1111/j.1745-6584.2011.00882.x

Carrillo, G., Troch, P. A., Sivapalan, M., Wagener, T., Harman, C., & Sawicz, K. (2011). Catchment classification: hydrological analysis of catchment behavior through process-based modeling along a climate gradient. *Hydrology and Earth System Sciences*, *15*(11), 3411–3430. https://doi.org/10.5194/hess-15-3411-2011

Carroll, R. W. H., Bearup, L. A., Brown, W., Dong, W., Bill, M., & Willlams, K. H. (2018). Factors controlling seasonal groundwater and solute flux from snow-dominated basins. *Hydrological Processes*, *32*(14), 2187–2202. https://doi.org/10.1002/hyp.13151

CGIAR-CSI. (2019, January 24). Global Aridity Index and Potential Evapotranspiration Climate Database v2. Retrieved August 22, 2020, from https://cgiarcsi.community/2019/01/24/global-aridity-index-and-potential-evapotranspiration-climate-database-v2/

Chaney, N. W., Van Huijgevoort, M. H. J., Shevliakova, E., Malyshev, S., Milly, P. C. D., Gauthier, P. P. G., & Sulman, B. N. (2018). Harnessing big data to rethink land

https://doi.org/10.5194/hess-2021-520
Preprint. Discussion started: 26 October 2021

heterogeneity in Earth system models. *Hydrology and Earth System Sciences*, *22*(6), 3311–3330. https://doi.org/10.5194/hess-22-3311-2018

Condon, L. E., Maxwell, R. M., & Gangopadhyay, S. (2013). The impact of subsurface conceptualization on land energy fluxes. *Advances in Water Resources*, *60*, 188–203. https://doi.org/10.1016/j.advwatres.2013.08.001

Cosgrove, B. A., Lohmann, D., Mitchell, K. E., Houser, P. R., Wood, E. F., Schaake, J. C., et al. (2003). Real-time and retrospective forcing in the North American Land Data Assimilation System (NLDAS) project. *Journal of Geophysical Research: Atmospheres*, *108*(D22). https://doi.org/10.1029/2002JD003118

Dai, Y., Zeng, X., Dickinson, R. E., Baker, I., Bonan, G. B., Bosilovich, M. G., et al. (2003). The Common Land Model. *Bulletin of the American Meteorological Society*, *84*(8), 1013–1024. https://doi.org/10.1175/BAMS-84-8-1013

Daly, C., Halbleib, M., Smith, J. I., Gibson, W. P., Doggett, M. K., Taylor, G. H., et al. (2008). Physiographically sensitive mapping of climatological temperature and precipitation across the conterminous United States. *International Journal of Climatology*, *28*(15), 2031–2064. https://doi.org/10.1002/joc.1688

Devadoss, J., Falco, N., Dafflon, B., Wu, Y., Franklin, M., Hermes, A., et al. (2020). Remote Sensing-Informed Zonation for Understanding Snow, Plant and Soil Moisture Dynamics within a Mountain Ecosystem. *Remote Sensing*, *12*(17), 2733. https://doi.org/10.3390/rs12172733

Fan, Y., Clark, M., Lawrence, D. M., Swenson, S., Band, L. E., Brantley, S. L., et al. (2019). Hillslope Hydrology in Global Change Research and Earth System Modeling. *Water Resources Research*, *55*(2), 1737–1772. https://doi.org/10.1029/2018WR023903

https://doi.org/10.5194/hess-2021-520
Preprint. Discussion started: 26 October 2021

Hydrology and Earth System Sciences Discussions

Ferguson, I. M., & Maxwell, R. M. (2010). Role of groundwater in watershed response and land surface feedbacks under climate change. *Water Resources Research*, *46*(10). https://doi.org/10.1029/2009WR008616

Freeze, R. A., & Harlan, R. L. (1969). Blueprint for a physically-based, digitally-simulated hydrologic response model. *Journal of Hydrology*, *9*(3), 237–258. https://doi.org/10.1016/0022-1694(69)90020-1

Foster, L.M., Williams, K.H., Maxwell, R.M., 2020. Resolution matters when modeling climate change in headwaters of the Colorado River. Environ. Res. Lett. https://doi.org/10.1088/1748-9326/aba77f

van Genuchten, M. Th. (1980). A Closed-form Equation for Predicting the Hydraulic Conductivity of Unsaturated Soils1. *Soil Science Society of America Journal*, *44*(5), 892. https://doi.org/10.2136/sssaj1980.03615995004400050002x

Grabs, T., Seibert, J., Bishop, K., & Laudon, H. (2009). Modeling spatial patterns of saturated areas: A comparison of the topographic wetness index and a dynamic distributed model. *Journal of Hydrology*, *373*(1), 15–23. https://doi.org/10.1016/j.jhydrol.2009.03.031

Harman, C., & Sivapalan, M. (2009). A similarity framework to assess controls on shallow subsurface flow dynamics in hillslopes. *Water Resources Research*, *45*(1). https://doi.org/10.1029/2008WR007067

Hjerdt, K. N., McDonnell, J. J., Seibert, J., & Rodhe, A. (2004). A new topographic index to quantify downslope controls on local drainage. *Water Resources Research*, *40*(5). https://doi.org/10.1029/2004WR003130

Hubbard, S. S., Williams, K. H., Agarwal, D., Banfield, J., Beller, H., Bouskill, N., et al. (2018). The East River, Colorado, Watershed: A Mountainous Community Testbed for

Improving Predictive Understanding of Multiscale Hydrological–Biogeochemical Dynamics. *Vadose Zone Journal*, *17*(1), 180061. https://doi.org/10.2136/vzj2018.03.0061

IGBP. (2018). Global plant database published - IGBP [text]. Retrieved October 17, 2018, from http://www.igbp.net/news/news/news/globalplantdatabasepublished.5.1b8ae20512db692f2a6800014762.html

Jefferson, J. L., Gilbert, J. M., Constantine, P. G., & Maxwell, R. M. (2015). Active subspaces for sensitivity analysis and dimension reduction of an integrated hydrologic model. *Computers & Geosciences*, *83*, 127–138. https://doi.org/10.1016/j.cageo.2015.07.001

Kassambara, A. (2017). *Practical guide to cluster analysis in R: Unsupervised machine learning* (Vol. 1). Sthda.

Loritz, R., Kleidon, A., Jackisch, C., Westhoff, M., Ehret, U., Gupta, H., & Zehe, E. (2019). A topographic index explaining hydrological similarity by accounting for the joint controls of runoff formation. *Hydrology and Earth System Sciences*, *23*(9), 3807–3821. https://doi.org/10.5194/hess-23-3807-2019

Lyon, S. W., & Troch, P. A. (2007). Hillslope subsurface flow similarity: Real-world tests of the hillslope Péclet number. *Water Resources Research*, *43*(7). https://doi.org/10.1029/2006WR005323

Lyon, Steve W., & Troch, P. A. (2010). Development and application of a catchment similarity index for subsurface flow. *Water Resources Research*, *46*(3). https://doi.org/10.1029/2009WR008500

Maina, F. Z., & Siirila-Woodburn, E. R. (2020). The Role of Subsurface Flow on Evapotranspiration: A Global Sensitivity Analysis. *Water Resources Research*, *56*(7), e2019WR026612. https://doi.org/10.1029/2019WR026612

Maxwell, R. M. (2013). A terrain-following grid transform and preconditioner for parallel, large-scale, integrated hydrologic modeling. *Advances in Water Resources*, *53*, 109–117. https://doi.org/10.1016/j.advwatres.2012.10.001

Maxwell, R. M., & Miller, N. L. (2005). Development of a Coupled Land Surface and Groundwater Model. *Journal of Hydrometeorology*, *6*(3), 233–247. https://doi.org/10.1175/JHM422.1

McDonnell, J. J., & Woods, R. (2004). On the need for catchment classification. *Journal of Hydrology*, *299*, 2–3. https://doi.org/10.1016/j.jhydrol.2004.09.003

NEON dataset. (2020). Land Cover and Processes | NSF NEON | Open Data to Understand our Ecosystems. Retrieved May 7, 2020, from https://www.neonscience.org/data/data-themes/land-cover-processes

Noël, P., Rousseau, A. N., Paniconi, C., & Nadeau, D. F. (2014). Algorithm for Delineating and Extracting Hillslopes and Hillslope Width Functions from Gridded Elevation Data. *Journal of Hydrologic Engineering*, *19*(2), 366–374. https://doi.org/10.1061/(ASCE)HE.1943-5584.0000783

Oudin, L., Kay, A., Andréassian, V., & Perrin, C. (2010). Are seemingly physically similar catchments truly hydrologically similar? *Water Resources Research*, *46*(11). https://doi.org/10.1029/2009WR008887

Pribulick, C. E., Foster, L. M., Bearup, L. A., Navarre-Sitchler, A. K., Williams, K. H., Carroll, R. W. H., & Maxwell, R. M. (2016). Contrasting the hydrologic response due to land cover and climate change in a mountain headwaters system. *Ecohydrology*, *9*(8), 1431–1438. https://doi.org/10.1002/eco.1779

https://doi.org/10.5194/hess-2021-520
Preprint. Discussion started: 26 October 2021

Hydrology and Earth System Sciences
Open Access
Discussions

Rahman, M., Sulis, M., & Kollet, S. J. (2016). Evaluating the dual-boundary forcing concept in subsurface–land surface interactions of the hydrological cycle. *Hydrological Processes*, *30*(10), 1563–1573. https://doi.org/10.1002/hyp.10702

Richards, L. A. (1931). Capillary conduction of liquids through porous medium. *Journal of Applied Physics*, *1*(5), 318–333. https://doi.org/10.1063/1.1745010

Ryken, A., Bearup, L. A., Jefferson, J. L., Constantine, P., & Maxwell, R. M. (2020). Sensitivity and model reduction of simulated snow processes: Contrasting observational and parameter uncertainty to improve prediction. *Advances in Water Resources*, *135*, 103473. https://doi.org/10.1016/j.advwatres.2019.103473

Sawicz, K., Wagener, T., Sivapalan, M., Troch, P. A., & Carrillo, G. (2011). Catchment classification: empirical analysis of hydrologic similarity based on catchment function in the eastern USA. *Hydrology and Earth System Sciences*, *15*(9), 2895–2911. https://doi.org/10.5194/hess-15-2895-2011

Schwanghart, W., & Scherler, D. (2014). Short Communication: TopoToolbox 2 – MATLAB-based software for topographic analysis and modeling in Earth surface sciences. *Earth Surface Dynamics*, *2*(1), 1–7. https://doi.org/10.5194/esurf-2-1-2014

SIVAPALAN, M., TAKEUCHI, K., FRANKS, S. W., GUPTA, V. K., KARAMBIRI, H., LAKSHMI, V., et al. (2003). IAHS Decade on Predictions in Ungauged Basins (PUB), 2003–2012: Shaping an exciting future for the hydrological sciences. *Hydrological Sciences Journal*, *48*(6), 857–880. https://doi.org/10.1623/hysj.48.6.857.51421

Wagener, T., Sivapalan, M., Troch, P., & Woods, R. (2007). Catchment Classification and Hydrologic Similarity. *Geography Compass*, *1*(4), 901–931. https://doi.org/10.1111/j.1749-8198.2007.00039.x

https://doi.org/10.5194/hess-2021-520
Preprint. Discussion started: 26 October 2021

Wainwright, H. M., Uhlemann, S., Franklin, M., Falco, N., Bouskill, N. J., Newcomer, M., Dafflon, B., Woodburn, E., Minsley, B. J., Williams, K. H., and Hubbard, S. S. (2021). Watershed zonation approach for tractably quantifying above-and-belowground watershed heterogeneity and functions, *Hydrol. Earth Syst. Sci. Discuss. [preprint], https://doi.org/10.5194/hess-2021-228, in review*.